

CoV₂O₆ Single Crystals Grown in a Closed Crucible: Unusual Magnetic Behaviors with Large Anisotropy and 1/3 Magnetization Plateau

Zhangzhen He,^{*,†} Jun-Ichi Yamaura,[‡] Yutaka Ueda,[‡] and Wendan Cheng^{*,†}

State Key Laboratory of Structural Chemistry, Fujian Institute of Research on the Structure of Matter (FIRSM), Chinese Academy of Sciences, Fuzhou, Fujian 350002, China, and Institute for Solid State Physics (ISSP), University of Tokyo, Kashiwa Chiba 277-8581, Japan

Received April 2, 2009; E-mail: hcz1988@hotmail.com; cwd@fjirsm.ac.cn

Transition-metal oxides with a linear chain structure have attracted much attention in solid-state physics and chemistry since the discovery of their various fascinating magnetic phenomena. Major interest in linear-chain systems is currently focused on the investigation of magnetic ground states that depend on magnetic ions with low spin values. For $S = 1/2$ systems, many copper- and vanadium-based oxides such as CuGeO₃,¹ BaCu₂V₂O₈,² (VO)₂P₂O₇,³ and NaV₂O₅⁴ are found to exhibit a spin-singlet ground state with a finite spin gap due to their strong quantum spin fluctuations. For $S = 1$ systems, nickel oxides including PbNi₂V₂O₈,⁵ SrNi₂V₂O₈,⁶ and Y₂BaNiO₅⁷ are also found to have a nonmagnetic ground state and serve as typical examples of the realization of Haldane's conjecture.⁸ For $S = 3/2$ systems, almost all cobalt oxides, such as BaCo₂Si₂O₇,⁹ CoNb₂O₆,¹⁰ and BaCo₂V₂O₈,¹¹ show a three-dimensional (3D) Neel ordering at low temperature. Besides magnetic ground states, field-induced quantum phase transitions are also one of the most promising features of spin-chain systems. For a spin-gap system, field-induced magnetic ordering can occur when a high enough magnetic field is applied. Such a quantum phase transition has been observed in PbNi₂V₂O₈.¹² On the other hand, cobalt oxides usually exhibit large magnetic anisotropy and also show interesting field-induced magnetic transitions. For example, an unusual spin-flop transition has been observed in CoNb₂O₆,¹⁰ while an order–disorder transition has been realized in BaCo₂V₂O₈.¹³

One cobalt oxide, CoV₂O₆,¹⁴ crystallizes in the monoclinic structure of space group C121 with $a = 9.256$ Å, $b = 3.508$ Å, $c = 6.626$ Å, and $\beta = 111.55^\circ$. As shown in Figure 1a, one of the most remarkable structural features is that magnetic Co²⁺ ions are equivalent to arrays of edge-shared CoO₆ octahedra forming linear chains, while nonmagnetic V⁵⁺ ions in VO₅ square pyramids form zigzag chains by sharing their basal edges along the b axis, resulting in a quasi-one-dimensional (1D) structural arrangement. In this communication, we report the growth of CoV₂O₆ crystals in a closed crucible and the observation of unusual magnetic behaviors of CoV₂O₆ that are clearly different from those in the linear-chain systems mentioned above.

A polycrystalline sample of CoV₂O₆ was synthesized by a standard solid-state reaction method using a mixture of high-purity CoC₂O₄·2H₂O (2N) and V₂O₅ (3N) reagents in a 1:1 molar ratio. The mixture was carefully ground to homogeneity with ethanol (99%) in an agate mortar and then calcined in an alumina crucible at 600 °C for 40 h with several intermediate grindings. Crystal growth of CoV₂O₆ was carried out in a commercial electric furnace. Since CoV₂O₆ exhibits an incongruent melting feature on the basis of the phase diagram of CoO–V₂O₅ systems,¹⁵ the flux method

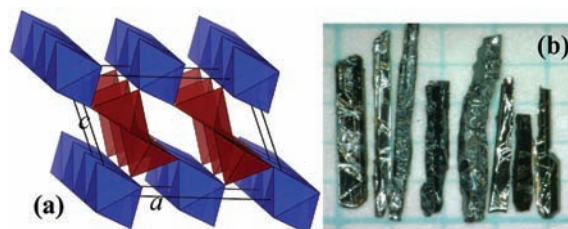


Figure 1. (a) Crystal structure of CoV₂O₆. Blue octahedra and red square pyramids represent CoO₆ and VO₅, respectively. (b) Single crystals of CoV₂O₆ grown in a closed crucible using the flux method.

was suitable for the growth of single crystals. To avoid impurities from the flux in the grown crystals, we selected one of starting materials, V₂O₅, to be self-fluxed. A mixture of polycrystalline CoV₂O₆ and V₂O₅ in a ratio of 3:2, which corresponds to a 3:5 CoO/V₂O₅ ratio, was melted in an alumina crucible ($\Phi 42 \times 50$ mm³), and then the crucible was capped with a cover using Al₂O₃ cement (C-989, Cotronics Corp.). The closed crucible was placed into the furnace, which was then heated to 780 °C and kept at that temperature for 20 h to ensure that the solution would melt completely and homogeneously. The furnace was slowly cooled to 600 °C at a rate of 1 °C/h and then cooled to room temperature at a rate of 100 °C/h. With this procedure, CoV₂O₆ crystals with needle morphology (Figure 1b) were obtained by mechanical separation from the crucible.

Recently, we successfully grew some vanadium oxides by the flux method.^{16–18} To grow large CoV₂O₆ single crystals with high quality, the following important points of the growth process should be noted: To allow slow, spontaneous nucleation in the melt, a very slow cooling rate is suitable for the growth. Further, to avoid the inclusion of the melt into the crystal by overcooling of the melt, the furnace must be kept at a constant temperature several times in the cooling process. In addition, to carefully avoid the evaporation of V₂O₅ at high temperature, which would result in an unsteady solution system during the growth, the alumina crucible must be capped with a cover using Al₂O₃ cement to form a closed system.

The quality of the grown crystal was analyzed by powder X-ray diffraction (XRD) and electron probe microanalysis (EPMA) techniques. XRD data for the crushed grown crystal was collected at room temperature using an MXPI8AHF X-ray diffractometer with graphite-monochromatized Cu K α radiation. It was found that all of the peaks in the XRD pattern obtained using the crushed crystals could be indexed with the monoclinic system and identified with the diffraction peaks of CoV₂O₆ (ICSD code 46003). The lattice constants of $a = 9.220(7)$ Å, $b = 3.494(3)$ Å, $c = 6.601(5)$ Å, and $\beta = 111.71(3)^\circ$ determined by using a high-purity Si powder as an internal standard are in good agreement with those reported previously.¹⁴ Chemical analysis via energy-dispersive spectroscopy

[†] FIRSM.

[‡] ISSP.

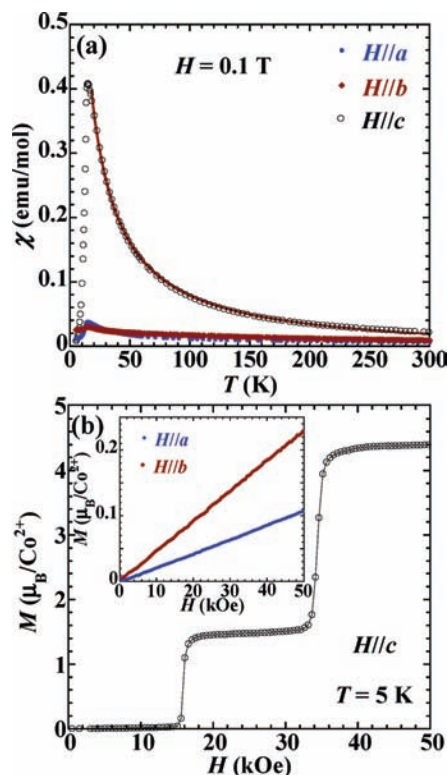


Figure 2. (a) Temperature dependence of the magnetic susceptibilities of CoV_2O_6 along the crystallographic a , b , and c axes. The solid line is a fit using an Ising spin chain model for Co^{2+} magnetic systems.¹⁹ (b) Magnetization measured as a function of the applied field H along the c and (inset) a and b axes at 5 K.

performed using an EPMA system indicated no other metal elements except for Co and V in these crystals. The results clearly show that the grown crystals have high quality.

The crystallographic axes of the grown crystals were determined using a Bruker SMART three-circle diffractometer equipped with a CCD area detector. The magnetic susceptibility was measured with an applied field of 0.1 T from 5 to 300 K, and the magnetization was measured at 5 K under applied fields from 0 to 5 T using a superconducting quantum interference device magnetometer (MPMS5S, Quantum Design). Figure 2a demonstrates the temperature dependence of the magnetic susceptibilities along the crystallographic a , b , and c axes. The susceptibilities increased with decreasing temperature, while a sharp peak was observed at ~ 14 K, indicating the onset of antiferromagnetic (AF) ordering. We note that the decrease in susceptibility below 14 K for $H \parallel c$ is more rapid than that for $H \parallel a$ or $H \parallel b$, showing that the c axis is the magnetic easy axis. We also note the large difference between the susceptibilities along the a or b axis and the c axis, which persists even up to room temperature, indicative of a large magnetic anisotropy in the system. In addition, the susceptibility above 14 K along the c axis can be fit well using an Ising spin chain model for Co^{2+} (d^7) magnetic systems,¹⁹ giving $J/k_B = -4.86(6)$ K and $g = 10.1(1)$, the value of which also indicates an unusual magnetic anisotropy.

The anisotropic AF feature of CoV_2O_6 was also confirmed through field-dependent magnetization measurements below 14 K. A linear increase in the magnetization was observed at 5 K along the a and b axes (Figure 2b inset), agreeing with an AF ordering

below 14 K. However, a staircase magnetization curve was clearly observed when the field was applied along the c axis (Figure 2b), with the first jump in the magnetization observed at ~ 1.6 T and the second one at ~ 3.3 T. With increasing magnetic field, the magnetization saturated completely at 4 T, and the ferromagnetic moment was roughly estimated to be $\sim 4.4 \mu_B/\text{Co}^{2+}$, which is much larger than the spin-only value of $3.0 \mu_B/\text{Co}^{2+}$ for the full moments of Co^{2+} ions. This indicates that the Co^{2+} ions in CoV_2O_6 are in a high-spin state and exhibit a large orbital moment contribution in the oxygen octahedral environment. We note that the spin moment of $\sim 1.47 \mu_B/\text{Co}^{2+}$, which corresponds to a $1/3$ saturation moment of $\sim 4.4 \mu_B/\text{Co}^{2+}$, is observed in the applied fields between 1.6 and 3.3 T. This shows the occurrence of a plateau at $1/3$ magnetization. Further, the applied field for the second jump in magnetization was ~ 2 times as large as that for the first one, also indicating an interesting quantum phase transition in the system.

Ising spin systems have been studied intensively in past decades.²⁰ It is well-known that a field-induced $1/3$ magnetization plateau can occur in frustrated Ising spin systems with a triangular lattice. Such magnetic behavior has been observed in some hexagonal systems, such as $\text{Ca}_3\text{Co}_2\text{O}_6$ ²¹ and $\text{SrCo}_6\text{O}_{11}$.²² However, we note that monoclinic CoV_2O_6 does not exhibit a triangular lattice as a structural feature.¹⁴ Therefore, we suggest that the $1/3$ magnetization plateau observed in CoV_2O_6 may arise from the unusual competition between interchain antiferromagnetic and ferromagnetic interactions, which is similar to that in a triangular structural lattice.

Acknowledgment. This work was partly supported by the National Natural Science Foundation of China under Project 20773131, the National Basic Research Program of China (2007CB815307), and Fujian Key Laboratory of Nanomaterials (2006L2005).

References

- (1) Hase, M.; Terasaki, I.; Uchinokura, K. *Phys. Rev. Lett.* **1993**, *70*, 3651.
- (2) He, Z.; Kyomen, T.; Itoh, M. *Phys. Rev. B* **2004**, *69*, 220407.
- (3) Barnes, T.; Riera, J. *Phys. Rev. B* **1994**, *50*, 6817.
- (4) Isobe, M.; Ueda, Y. *J. Phys. Soc. Jpn.* **1996**, *65*, 1178.
- (5) Uchiyama, Y.; Sasago, Y.; Tsukada, I.; Uchinokura, K.; Zheludev, A.; Hayashi, T.; Miura, N.; Böni, P. *Phys. Rev. Lett.* **1999**, *83*, 632.
- (6) Pahari, B.; Ghoshray, K.; Sarkar, R.; Bandyopadhyay, B.; Ghoshray, A. *Phys. Rev. B* **2006**, *73*, 012407.
- (7) Xu, G.; DiTusa, J. F.; Ito, T.; Oka, K.; Takagi, H.; Broholm, C.; Aeppli, G. *Phys. Rev. B* **1996**, *54*, R6827.
- (8) Haldane, F. D. M. *Phys. Rev. Lett.* **1983**, *50*, 1153.
- (9) Adams, R. D.; Layland, R.; Payen, C.; Datta, T. *Inorg. Chem.* **1996**, *35*, 3492.
- (10) Kobayashi, S.; Mitsuda, S.; Ishikawa, M.; Miyatani, K.; Kohn, K. *Phys. Rev. B* **1999**, *60*, 3331.
- (11) He, Z.; Fu, D.; Kyömen, T.; Taniyama, T.; Itoh, M. *Chem. Mater.* **2005**, *17*, 2924.
- (12) Tsujii, N.; Suzuki, O.; Suzuki, H.; Kitazawa, H.; Kido, G. *Phys. Rev. B* **2005**, *72*, 104402.
- (13) He, Z.; Kyömen, T.; Taniyama, T.; Itoh, M. *Phys. Rev. B* **2005**, *72*, 172403.
- (14) Jasper-Toennies, B.; Mueller-Buschbaum, H. *Z. Anorg. Allg. Chem.* **1984**, *508*, 7.
- (15) Levin, E. M.; Robbins, C. R.; Mcmurdie, H. F. *Phase Diagrams for Ceramists*; American Ceramic Society: Westerville, OH, 1964; Vol. 1, No. 55.
- (16) He, Z.; Ueda, Y.; Itoh, M. *J. Cryst. Growth* **2006**, *297*, 1.
- (17) He, Z.; Taniyama, T.; Itoh, M.; Ueda, Y. *Cryst. Growth Des.* **2007**, *7*, 1055.
- (18) He, Z.; Ueda, Y. *J. Cryst. Growth* **2008**, *310*, 171.
- (19) Rohrs, B. R.; Hatfield, W. E. *Inorg. Chem.* **1989**, *28*, 2772.
- (20) Achiwa, N. *J. Phys. Soc. Jpn.* **1969**, *27*, 561.
- (21) Kageyama, H.; Yoshimura, K.; Kosuge, K.; Mitamura, H.; Goto, T. *J. Phys. Soc. Jpn.* **1997**, *66*, 1607.
- (22) Ishiwata, S.; Wang, D.; Saito, T.; Takano, M. *Chem. Mater.* **2005**, *17*, 2789.

JA902623B